

Adversarial Hubness in Multi-Modal Retrieval

Tingwei Zhang[†] Fnu Suya[§] Rishi Jha[†] Collin Zhang[†] Vitaly Shmatikov[†]

[†]Cornell Tech [§]University of Tennessee, Knoxville

tingwei@cs.cornell.edu suya@utk.edu {rjha, collinzhang, shmat}@cs.cornell.edu

Abstract—Hubness is a phenomenon in high-dimensional vector spaces where a single point from the natural distribution is unusually close to many other points. This is a well-known problem in information retrieval that causes some items to accidentally (and incorrectly) appear relevant to many queries.

In this paper, we investigate how attackers can exploit hubness to turn any image or audio input in a multi-modal retrieval system into an adversarial hub. Adversarial hubs can be used to inject universal adversarial content (e.g., spam) that will be retrieved in response to thousands of different queries, as well as for targeted attacks on queries related to specific, attacker-chosen concepts.

We present a method for creating adversarial hubs and evaluate the resulting hubs on benchmark multi-modal retrieval datasets and an image-to-image retrieval system based on a tutorial from Pinecone, a popular vector database. For example, in text-caption-to-image retrieval, a single adversarial hub is retrieved as the top-1 most relevant image for more than 21,000 out of 25,000 test queries (by contrast, the most common natural hub is the top-1 response to only 102 queries). We also investigate whether techniques for mitigating natural hubness are an effective defense against adversarial hubs, and show that they are not effective against hubs that target queries related to specific concepts.

1. Introduction

Cross-modal and multi-modal retrieval systems that enable flexible and accurate information retrieval across different modalities (e.g., text-to-image, image-to-image, and text-to-audio) have drawn significant attention in recent years [61], [62]. Modern retrieval systems leverage pre-trained multi-modal encoders, such as ImageBind [21] and AudioCLIP [23]. Inputs from different modalities (e.g., images and texts) are encoded into the same embedding space, with semantically related inputs clustered together (see Section 2 for details). Queries are encoded into the same space, and retrieval is based on similarity between query embeddings and input embeddings [48]. Embedding-based retrieval is more scalable and accurate than traditional techniques based on metadata or keywords [3], [28].

High-dimensional embedding spaces are prone to *hubness* [46], one of the manifestations of the curse of dimensionality. Hubness is a phenomenon where a point (a “natural hub”) appears in the neighborhood of many other

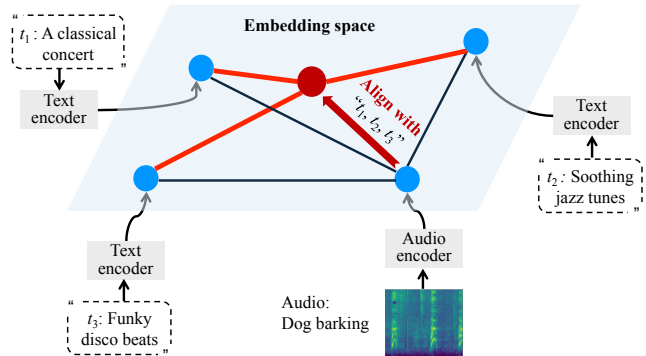


Figure 1: Cross-modal adversarial hub in the embedding space.

points to which it is not semantically related. Hubness exists in many high-dimensional natural distributions and is a well-known problem in the information retrieval literature [38], [46]. Many methods have been proposed for mitigating natural hubness [25], [27], [49], [49], [58], [69], and there is a growing interest in methods specifically for multi-modal retrieval [4], [13], [63], which is more vulnerable to hubness than single-modality retrieval [34].

In this paper, we investigate whether hubness can be exploited by adversaries to intentionally create images and audio inputs that act as “adversarial hubs.” Adversarial hubs (1) carry adversarial content, e.g., spam or misinformation, and (2) are very close in the embedding space to many queries in the same or different modality, causing them to be retrieved in response to these queries. For example, Figure 1 shows that a mild perturbation can align an audio clip of a barking dog to many unrelated text captions, including “A classical concert”, “Soothing jazz tunes”, and “Funky disco beats”, causing it to be retrieved whenever users search for any of these music genres. Figures 2, 3 and 4 illustrate concrete examples of adversarial hubs for different cross-modal retrieval scenarios.

Prior research on vulnerabilities in embedding-based retrieval focused on targeted adversarial alignment [71], poisoning of text-only retrieval corpora [10], [74], and uni-modal adversarial hubs in music recommendation [25]. There is also a substantial literature on multi-modal adversarial examples whose objectives are related to downstream models rather than embeddings, such as jailbreaking LLM generation and causing misclassification of multi-modal in-

puts (Section 7). Adversarial hubs is the first cross-modal attack that targets retrieval *and* affects multiple queries at the same time—either all queries, or the subset of queries related to a specific concept.

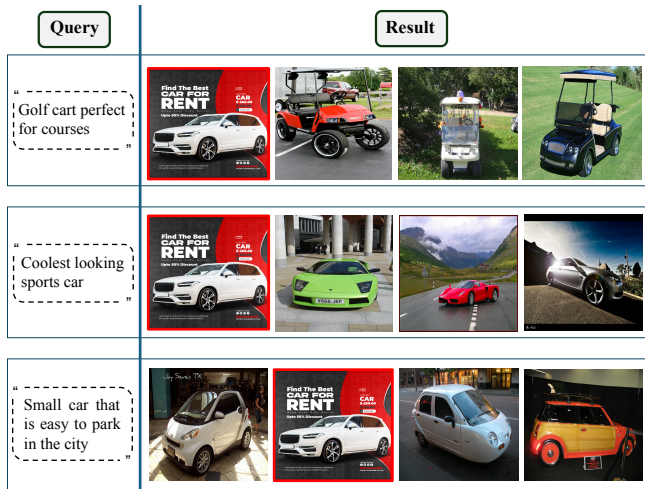


Figure 2: Illustration of an adversarial hub in text-to-image retrieval.

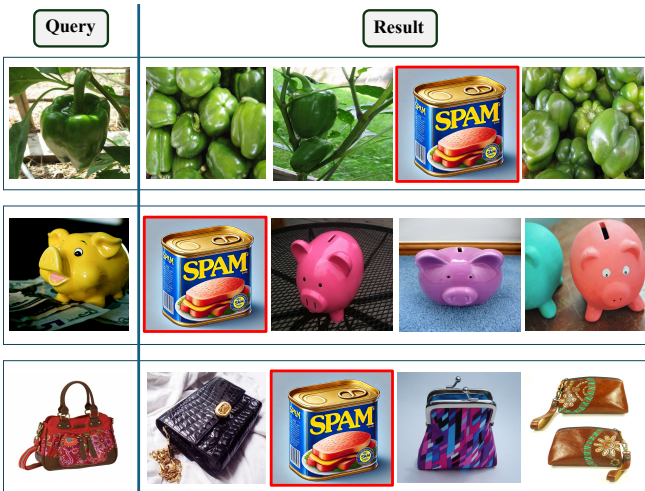


Figure 3: Illustration of an adversarial hub in image-to-image retrieval.

Our contributions. First, we show that hubness—a natural phenomenon in high-dimensional spaces where only a few data points become natural hubs—can be adversarially exploited. We demonstrate that attackers can apply a small perturbation, generated with standard techniques, to any image or audio input with an attacker-chosen semantics (e.g., an advertisement, a product promotion, a song, etc.) to turn this input into an adversarial hub that will be retrieved in response to many queries in an embedding-based cross-modal retrieval system.

Second, we show that a single adversarial hub can affect a large number of semantically unrelated queries,

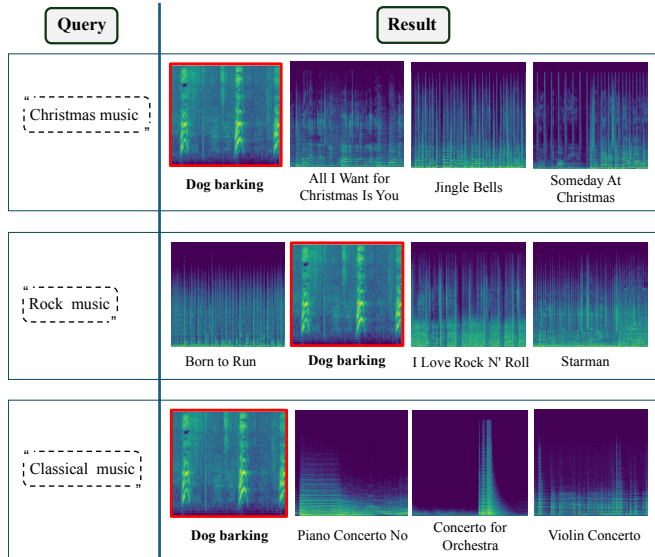


Figure 4: Illustration of an adversarial hub in text-to-audio retrieval.

significantly more than natural hubs. We also show that the attack can target specific concepts, so that the hub is retrieved only in response to queries related to that concept but not other queries. We evaluate these attacks on the same benchmarks as prior work [4], [13], [63], and also on a realistic image-to-image retrieval system based on a Pinecone tutorial [1]. We further investigate whether hubs generated for one embedding space transfer to another, and demonstrate some transferability across embedding models based on similar architectures.

Third, we evaluate existing techniques for mitigating natural hubness and show that they fail to mitigate concept-specific adversarial hubs even if hub generation is oblivious of the defense.

Our results highlight a new risk to embedding-based, multi-modal retrieval systems, and we hope that they will motivate research on adversarially robust multi-modal embeddings.

To facilitate research on the security of multi-modal embeddings, we released our code and models ¹.

2. Multi-Modal Retrieval

Traditional retrieval systems relied on hand-crafted features and metadata. Hand-crafted features, such as SIFT and color histograms for images [39] and TF-IDF for text [47], provided basic representations that captured low-level information. Metadata, such as tags, labels, or captions, was leveraged to bridge different modalities by aligning co-occurring information, as seen in early image annotation systems [3], [28].

With the rise of deep learning, the field shifted toward models such as CLIP [45], pretrained on massive datasets to

1. https://github.com/Tingwei-Zhang/adv_hub

produce embeddings, which are dense vector representations of inputs. Embeddings map semantically related inputs from the same or different modalities (e.g., images and texts) into a shared latent space, greatly improving accuracy for both single-modality and cross-modal retrieval tasks. Typically, encoders into the embedding space are trained to minimize cosine similarity between related inputs, which helps ensure that their embeddings are neighbors and thus improve cross-modal retrieval performance [50].

Multi-modal Embeddings. A multi-modal encoder θ^m transforms inputs from some modality $m \in \mathcal{M}$ into a common embedding space. In our evaluation, we primarily focus on systems with two modalities, but extending to more modalities is straightforward: generate bi-modal input pairs for different modality combinations and train as below.

Given a bi-modal dataset $D = (X, Y) \in m_1 \times m_2$, where (x, y) are semantically aligned (for instance, an image of a car and the text caption “Cars”), contrastive learning [42] is used to train the encoders by bringing representations of the aligned pairs closer in the embedding space while pushing apart representations of unaligned inputs.

Cross-modal Retrieval. Consider an image retrieval system, consisting of (1) a vector database with image embeddings that acts as a “Gallery”, and (2) “Queries” submitted by users in order to retrieve relevant images from the gallery. Queries can be in the same or different modality as the gallery. In text-to-image retrieval, queries are text captions (e.g., descriptions of cats), whereas in image-to-image retrieval queries are images (e.g., cat pictures). We use m_1 to denote the modality of queries and m_2 to denote the modality of the gallery data. Let $Q = \{q_i\}_{i=1}^N$ denote the queries, $G = \{g_i\}_{i=1}^S$ be the vectors corresponding to the gallery data. Let $\theta^{m_1}(\cdot)$ be the encoder for queries, $\theta^{m_2}(\cdot)$ for the gallery.

The retrieval system encodes the query and measures the cosine similarity of the resulting embedding with each data point in the gallery $g_j \in G$ as

$$\text{sim}(q_i, g_j) = \cos(\theta^{m_1}(q_i), \theta^{m_2}(g_j)),$$

then ranks all gallery data points from high to low based on their similarity to q_i , $\text{sort}(\text{sim}(q_i, g_1), \dots, \text{sim}(q_i, g_S))$, and finally returns the top k most relevant gallery data points.

3. Threat Model and Attack Methods

We describe the attacker’s goals (Section 3.1), then their knowledge and capabilities (Section 3.2), and then present the adversarial hubness attack in Section 3.3.

3.1. Attacker’s Goals

Figure 5 shows an overview of the threat model. The attacker aims to inject a maliciously crafted input g_a into the gallery that will act as an “adversarial hub” in the following sense. When a user submit a query, in the same or different modality as the gallery, the retrieval system will

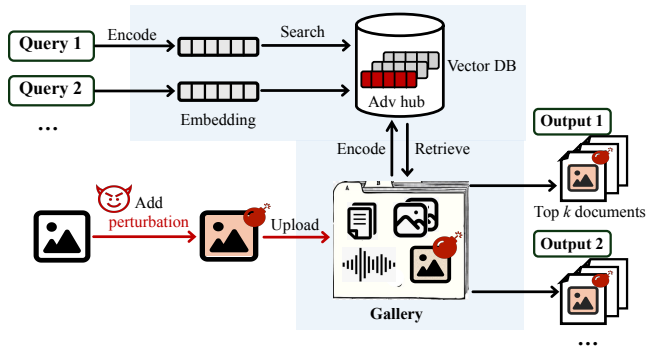


Figure 5: Attacking retrieval system with an adversarial hub.

compute the cosine similarities between the query and the embeddings of all gallery inputs. The embedding of the adversarial hub should appear as one of the most relevant, i.e., closest in the embedding space, to the embedding of the query. Furthermore, this has to be the case for many unrelated queries, even though the content of g_a is irrelevant to them.

Types of Adversarial Hubs. We consider two types of adversarial hubs: (1) *rational* hubs, which have semantics (i.e., human-understandable meaning) and can be driven by economic or other incentives, such as promoting products or songs, spreading misinformation, etc.; and (2) *reckless* hubs, which lack semantic meaning and aim solely to cause a denial-of-service impact on retrieval performance. In the rest of this paper, we focus primarily on rational hubs, since they are associated with practical threats to real-world retrieval systems. Our techniques for generating adversarial hubs work the same for either hub type.

Injecting adversarial hubs is straightforward when galleries contain user-generated data. For example, an attacker can post a hub online and wait for it to be indexed or added by users into their galleries [7]. In e-commerce applications, the attacker can include the hub in their product description. We focus on attacks involving a single adversarial hub, but in practice an attacker can control multiple inputs [77].

We consider two adversarial objectives: (1) *indiscriminate* attacks that aim to impact all queries, and (2) *concept-specific* attacks that aim to impact only certain queries. Both types of hubs can be used for both objectives.

Indiscriminate Objective. The indiscriminate attack is universal: it aims to ensure that the adversarial hub is close to as many queries as possible (all of them irrelevant to the semantic content of the hub, which is freely chosen by the adversary). For example, in a text-to-image retrieval system, an adversarial image hub will be retrieved in response to captions such as “cars”, “food”, “house”, etc. Similarly, in a text-to-audio retrieval system, regardless of what type of music the user searches for, the adversary’s audio will be retrieved as one of the most relevant songs. In this sense, adversarial hubs behave like natural hubs, except that they

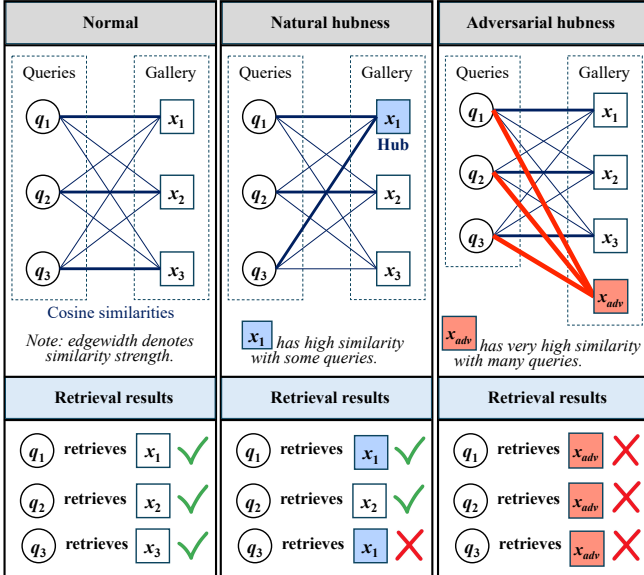


Figure 6: Natural hubs and adversarial hubs.

are retrieved much more frequently (see Figure 6).

Concept-specific Objective. We also consider a stealthier, concept-specific attack, where the attacker’s goal is to have their content retrieved only in response to queries related to a certain *concept* (e.g., specific keywords like car make and model or broader concepts like “cars”) and *not* retrieved in response to unrelated queries. For example, in text-to-audio retrieval, the attacker can create an audio that is retrieved only when users search for “country” or “jazz.”

The concept-specific attack is superficially similar to attacks on retrieval-augmented generation [10] that target queries with a certain trigger word, but those attacks are currently limited to text-to-text retrieval and require that the adversarial documents contain gibberish text whose embedding is close to the trigger.

Security Consequences of Adversarial Hubness. Adversarial hubs can be used to spread spam, or simply to degrade performance of retrieval systems thus causing denial of service. For example, in the music industry [19], [25] platforms like Spotify are constantly battling malicious actors who attempt to promote their content and manipulate platforms into streaming it for many users [55]. In online retail, hubness attacks could be used to manipulate product search. In social media, they could help propagate misinformation and amplify misleading content. These examples show that adversaries have an economic incentive to exploit hubness, thus it is important to develop robust mitigation strategies for retrieval systems that operate on user-generated content.

3.2. Attacker Knowledge and Capabilities

White-box Setting. In the white-box setting, the attacker knows all information about the victim system, including

the embedding models $\theta^{m_1}, \theta^{m_2}$ and a set of queries Q_t sampled from same distribution as the expected user queries. For the indiscriminate attack, Q_t contains samples from the entire distribution of user queries, while for concept-specific attack, Q_t contains samples from the distribution of queries related to a specific, attacker-chosen concept. The attacker does not need to know anything about the benign inputs in G (beyond basic information such as formatting, etc.) because adversarial hubs are independent of the existing gallery data points. White-box knowledge enables the attacker to back-propagate gradients with respect to the inputs and optimize the adversarial hub, as described in Equation (2)

The white-box assumption is common in the adversarial machine learning literature [40], [59]. It helps assess vulnerability of a system in the worst-case scenario, following the Kerckhoffs’s Principle [30].

Black-box Setting. We also consider the black-box setting where the attacker does not know the architecture of the embedding models used in the target retrieval system. In this setting, the attacker can use an available pretrained encoder and optimize an adversarial hub with respect to this surrogate, hoping that the resulting hub will *transfer* to the target encoder.

3.3. Generating Adversarial Hubs

We consider a cross-modal retrieval task where queries Q_t have modality m_1 and gallery data G have modality m_2 . The adversary’s goal is to generate an adversarial hub g_a in modality m_2 that is close to Q_t in the embedding space, so that when similar queries are submitted to the retrieval system, g_a will be retrieved in response.

To generate rational hubs, the attacker starts with an arbitrary input g_c in the same modality as the gallery G . g_c is completely independent from what is already in G and can carry arbitrary semantics, such as spam, a product promotion, a new song, etc. g_c is also irrelevant to (almost) all target queries Q_t . Then the attacker adds a (small) perturbation δ to g_c to produce an adversarial hub $g_a = g_c + \delta$, such that the embedding $\theta^{m_2}(g_a)$ is close to the embeddings of target queries $\{\theta^{m_1}(q) : q \in Q_t\}$.

We require the perturbation to be bounded with $\|\delta\|_\infty \leq \epsilon$. This bound serves two purposes: (1) keeping the perturbation small helps ensure that the input still has the human-perceived semantics desired by the adversary (e.g., the ad still contains information about the product, the audio clip is not heavily distorted, etc.), and (2) small perturbations are less likely to be detected by inspectors who may want to manually remove abnormal inputs from the gallery (e.g., a song that sounds like noise) [51], nor by users who receive the results of retrieval.

If the attacker’s goal is to generate a “reckless” hub that aims simply to degrade performance of the target retrieval system, the perturbation need not be bounded. Therefore, the norm constraint can be dropped when generating the hub, resulting in an even stronger attack.

For notational convenience, we let $\theta = (\theta^{m_1}, \theta^{m_2})$. To generate an adversarial hub, the attacker needs to optimize δ by solving the following constrained optimization problem:

$$\begin{aligned} \arg \min_{\delta} [\mathcal{L}(g_a, Q_t; \theta) = \mathcal{L}(g_c + \delta, Q_t; \theta)] \\ \text{s.t. } \|\delta\|_{\infty} \leq \epsilon, \end{aligned} \quad (1)$$

where

$$\mathcal{L}(g_a, Q; \theta) = 1 - \frac{1}{|Q_t|} \sum_{q \in Q_t} \cos(\theta^{m_2}(g_a), \theta^{m_1}(q)) \quad (2)$$

To optimize the objective above, we iteratively update perturbation δ using Projected Gradient Descent (PGD), which naturally handles the constraint $\|\delta\|_{\infty} \leq \epsilon$ through projection [40]. In the concept-specific attack, when Q_t only contains a subset of queries, we find that the above optimization is sufficient to create hubs that impact only these concepts without interfering with other queries (i.e., there is minimal collateral damage).

4. Experimental Setup

Datasets. Following the same setup as [4]: for the text-to-image retrieval task, we use the standard MS COCO [11] dataset; for the image-to-image task, we use the CUB-200-2011 [60], and for the text-to-audio task, we use AudioCaps [31]. Details of each dataset are below:

- *MS COCO* [11] is a widely used image captioning and image-to-text matching dataset. For our evaluation, we use its test set of 5,000 images as the gallery data and the associated 25,000 captions (5 each) as user queries. By default, we optimize the adversarial hub perturbation based on these user queries. However, to further demonstrate the generalization capability of our generated adversarial hubs, we additionally selected 5,000 random captions from the training set of MSCOCO, use them to form another set of test queries and report the retrieval performance.
- *CUB-200-2011* [60] is an image classification dataset consisting of various bird species. Using its test set, we randomly select one image from each of the 200 classes to form the gallery data, and use the remaining 5,724 images as user queries.
- *AudioCaps* [31] is a widely-used audio captioning dataset. We use its test set of 816 audios and corresponding text captions as gallery data and queries, respectively.

Models. We use the popular open-source encoders: ImageBind [21] (6 modalities), AudioCLIP [23] (3 modalities), and CLIP (2 modalities) [45]. For tasks involving images, we use a partially trained checkpoint of AudioCLIP, as it achieves better performance [23]. Our evaluations on CLIP are done on two sizes (ViT and ResNet-50) using the implementations provided by OpenCLIP [12].

Pinecone. In addition to evaluating the above models as “simulated” retrieval systems (following the previous litera-

ture [4], [63]), we also construct a more realistic setting by attacking Pinecone’s image-to-image retrieval application².

Based on Pinecone’s documentation, the application uses CLIP [45] to convert both user queries and gallery data to the embeddings, but does not specify the version number. Therefore, we assume the adversary does not know the exact version of CLIP, but has access to the models we included in other experiments. This assumption is realistic since training one’s own encoder is prohibitively expensive and potential victims often leverage leading open-source implementations. We also assume the adversaries have no control over the configurations of the Pinecone application other than uploading the gallery data, which closely mimics how a victim would build its own real-world retrieval system based on Pinecone. We test on the CUB-200-2011 dataset, using the same gallery and query set split as above.

Attack Setup. For each of our attacks, we only generate a single adversarial hub and add it to the gallery data to show the effectiveness of being retrieved by a large fraction of irrelevant test queries. To generate the adversarial hub, we randomly select a clean gallery point $g_c \in G$, optimize the perturbation δ based on (2) and run the PGD attack for $T = 1000$ iterations to obtain the adversarial hub $g_a = g_c + \delta$. We set the perturbation budget of δ as $\epsilon = 16/255$ for image and $\epsilon = 0.05$ for audio, following the prior work [71].

Evaluation Metrics. We use two standard retrieval metrics.

- *Recall at Rank k ($R@k$):* Given a query $q_i \in Q = \{q_i\}_{i=1}^N$, we calculate the number of relevant documents in the gallery, R_i , and number of relevant documents retrieved in the top- k list, R_i^k . Then,

$$R@k = \frac{1}{N} \sum_{i=1}^N \frac{R_i^k}{R_i} \times 100\%.$$

Higher values indicate better retrieval performance.

- *Median Rank (MdR):* For a query q_i , let r_i be the rank of the first relevant retrieved gallery datum in the ranked list of all gallery items. Then,

$$\text{MdR} = \text{median}(\{r_1, r_2, \dots, r_N\}).$$

Lower values indicate better retrieval performance.

Using the two evaluation metrics described above, for each evaluation setting, we first measure the retrieval performance of the relevant documents in the original *clean* gallery using the user queries (clean retrieval performance). Next, we inject the adversarial hub into the gallery to create a *poisoned* gallery and measure the performance again with the same set of queries. In the poisoned gallery, we report the retrieval performance of both the injected adversarial hub and the original relevant documents from the clean gallery.

Finally, we independently generate 100 adversarial hubs for images and audio, and report their statistics (mean and standard deviation) for both top- k recall ($R@k$) and median rank (MdR). An effective adversarial hub should achieve a very high $R@k$ and a low MdR when retrieved by targeted user queries.

2. <https://github.com/pinecone-io/image-search-example>

5. Evaluation Without Defenses

We evaluate the effectiveness of our universal adversarial hubs in the white-box setting in Section 5.1. We then compare our hubs with their natural counterparts in Section 5.2. Next, we evaluate the transferability of universal adversarial hubs across different embeddings in Section 5.3. Finally, we evaluate the effectiveness of our stealthier, concept-specific hubs in Section 5.4.

5.1. Effectiveness of Universal Adversarial Hubs

Text-to-Image Retrieval. Table 1 presents the text-to-image retrieval results for the ImageBind, OpenCLIP, and AudioCLIP models on the MS COCO dataset. With clean gallery data, we observe significant variance in performance across different embeddings, with OpenCLIP achieving the highest $R@k$ for $k = 1, 5, 10$ and lowest M $\bar{d}R$. Setting $k = 10$, each model achieves reasonably good performance with the best embedding (from OpenCLIP) achieving $R@10 > 81\%$ and $M\bar{d}R = 2$. However, when an adversarial hub is introduced to the gallery, the retrieval performance is significantly degraded across the board.

Our attack is highly effective, with $R@k \approx 100\%$ for most models and settings of k . Our lowest attack performance is on the partially-trained AudioCLIP model with $R@1 = 65.5\%$, however, we note that in this regime retrieval becomes unusable on the clean gallery data ($R@1 = 18.8\%$). For all other models, $M\bar{d}R = 1$, indicating that the single adversarial hub is the most relevant data point to (almost) all incoming queries: even though *the adversarial hub is semantically irrelevant* to those queries. We also note that, as k increases, the (truly) relevant points from the gallery are also retrieved more frequently, although still dominated by the adversarial hub in the retrieved rankings.

As explained before, by default, the generation of the adversarial hubs across all settings is based on the user queries in Q_t . To further show the generalization of the generated adversarial hubs, we test on queries that are sampled from the same distribution as Q_t , but were never used for hub optimization. In this evaluation, we randomly sample 5,000 text captions from the MS COCO dataset and use them as queries for retrieval. As shown in the table (last row for each model), the adversarial hub generalizes very well and the retrieval performance on the new test queries is almost the same as the performance on the target queries Q_t .

Image-to-Image Retrieval. Table 2 shows the image-to-image retrieval results on the CUB-200-2011 dataset using the same models as above and, additionally, on Pinecone’s retrieval system. While our main focus is on cross-modal retrieval, we evaluate image-to-image retrieval since it is common for many real-world applications such as Google’s “Search by Image” functionality.

Like text-to-image retrieval, we observe significant variance in image-to-image performance across models, with OpenCLIP achieving the highest $R@k$ for $k = 1, 3, 5, 10$

and lowest median rank. We note that OpenCLIP’s superior performance justifies why victim users in practice may deploy the (default) OpenCLIP when using Pinecone.

Interestingly, when compared to the text-to-image setting, both clean retrieval and our adversarial hubs are not nearly as effective. However, our attack performance improves with k and achieves $R@10 = 92.3\%$ on OpenCLIP-ViT. We remark that, in practice, larger values of k may be needed in this regime to boost clean recall and rank.

We also evaluate our attack performance on Pinecone (final row of Table 2). Since our attacker has no control over the internal configurations of the retrieval system (*e.g.*, the value of k), we only report results for $k \leq 5$ and omit the median rank $M\bar{d}R$ which requires a complete ranking of the gallery data. Our attack shows similar success to the “simulated” model settings, achieving $R@1 = 11.0\%$ and $R@5 = 45.7\%$. The effectiveness of clean retrieval and our attack still improves with larger k .

Since our attack performance is strongly correlated with clean retrieval performance, we note that adversarial hubs pose a significant threat even to relatively robust single-modality retrieval tasks, with the potential to harm real-world retrieval systems. We speculate that, compared to cross-modal tasks, single-modality tasks may have more compact representations, leaving less opportunity for manipulation by attackers. Similar observations of increased (natural) hubness in cross-modal retrieval compared to unimodal retrieval have also been reported in prior work [34].

Text-to-Audio Retrieval. Table 3 contains our text-to-audio retrieval results for ImageBind and AudioCLIP on the AudioCaps dataset. Even though the clean retrieval performance is low in the restrictive top-1 regime ($R@1 < 10\%$), our adversarial hubs can be reliably retrieved as the most relevant gallery point with $R@1 > 50\%$. As expected, as we increase k to improve clean retrieval, the effectiveness of the adversarial hub increases with $R@10 \approx 88\%$. For our hubs, $M\bar{d}R \approx 1.5$ while for clean retrieval the median rank is as high as 28.

These results suggest that audio embeddings are highly vulnerable to adversarial perturbations, as a single adversarial audio sample can align with a wide range of captions. However, when compared to text-to-image retrieval, text-to-audio alignment appears to be slightly more robust by both metrics. We expect that as clean retrieval scores improve, so, too, will our attack.

5.2. Comparing Adversarial and Natural Hubs

In Figure 7 we show the frequency of gallery points being retrieved as the most relevant (indicated by the width of the plots) for different numbers of queries (y-axis) across text-to-image, image-to-image, and text-to-audio retrieval tasks. At a particular number of queries on the y-axis, y , a wider plot means there are more gallery data points retrieved y times. As shown, the adversarial hub (in red) is retrieved as the most relevant gallery point an order of magnitude more frequently than any natural hub. On the MS

TABLE 1: **Result for Text-to-Image Retrieval(MS COCO)**. In column of “Gallery”, “Clean” denotes the original clean gallery for retrieval, “Poisoned” denotes the poisoned gallery that injects the adversarial hub to the original gallery; In column of “Retrieved”, “Relevant Doc.” denote relevant documents in the original clean gallery for the query. “Adv. Hub.” denotes the injected adversarial hub. The metric of $R@k$ denotes the top- k recall of the retrieved document (Retrieved) and MdR denotes the median rank of the retried document in the complete rank of the gallery. We report the performance of retrieving relevant documents (Relevant Doc.) from both the Clean and Poisoned gallery, and the retrieval iof adversarial hub (Adv Hub.) from the Poisoned gallery. “(Test Queries)” in the last row of each “Model” denotes retrieval of adversarial hub using queries not used for its optimization. The attack performance is shaded. We report the average and standard deviation of all metrics over 100 independently generated adversarial hubs.

Model	Gallery	Retrieved	$R@1$ (%) \uparrow	$R@5$ (%) \uparrow	$R@10$ (%) \uparrow	MdR \downarrow
ImageBind	Clean	Relevant Doc.	48.4	72.7	81.0	2.0
	Poisoned	Relevant Doc.	9.2 \pm 2.1	69.6 \pm 0.0	79.8 \pm 0.0	3.0 \pm 0.0
	Poisoned	Adv. Hub	87.7 \pm 3.0	98.5 \pm 0.5	99.2 \pm 0.3	1.0 \pm 0.0
	Poisoned	Adv. Hub (Test Queries)	94.9 \pm 1.6	98.5 \pm 0.5	99.2 \pm 0.3	1.0 \pm 0.0
AudioCLIP	Clean	Relevant Doc.	13.4	31.5	41.7	16.0
	Poisoned	Relevant Doc.	0.0 \pm 0.0	28.3 \pm 0.0	40.0 \pm 0.0	17.0 \pm 0.0
	Poisoned	Adv. Hub	99.9 \pm 0.1	100.0 \pm 0.0	100.0 \pm 0.0	1.0 \pm 0.0
	Poisoned	Adv. Hub (Test Queries)	100.0 \pm 0.1	100.0 \pm 0.0	100.0 \pm 0.0	1.0 \pm 0.0
OpenCLIP-ViT	Clean	Relevant Doc.	48.5	72.8	81.1	2.0
	Poisoned	Relevant Doc.	9.3 \pm 1.8	69.7 \pm 0.1	79.8 \pm 0.0	3.0 \pm 0.1
	Poisoned	Adv. Hub	87.7 \pm 2.7	98.5 \pm 0.5	99.2 \pm 0.3	1.0 \pm 0.0
	Poisoned	Adv. Hub (Test Queries)	97.4 \pm 1.5	99.2 \pm 0.5	99.6 \pm 0.3	1.0 \pm 0.0
OpenCLIP-RN50	Clean	Relevant Doc.	28.3	53.0	64.1	5.0
	Poisoned	Relevant Doc.	2.2 \pm 0.8	49.3 \pm 0.0	62.4 \pm 0.0	6.0 \pm 0.0
	Poisoned	Adv. Hub	95.9 \pm 2.0	99.0 \pm 0.6	99.5 \pm 0.3	1.0 \pm 0.0
	Poisoned	Adv. Hub (Test Queries)	94.9 \pm 1.5	98.5 \pm 0.4	99.2 \pm 0.3	1.0 \pm 0.0
AudioCLIP (Partial)	Clean	Relevant Doc.	18.8	39.5	50.7	10.0
	Poisoned	Relevant Doc.	8.2 \pm 3.6	36.8 \pm 0.4	49.2 \pm 0.2	11.0 \pm 0.1
	Poisoned	Adv. Hub	65.5 \pm 19.1	83.9 \pm 13.2	89.3 \pm 10.3	1.6 \pm 2.6
	Poisoned	Adv. Hub (Test Queries)	69.0 \pm 18.5	84.8 \pm 12.8	89.9 \pm 10.0	1.5 \pm 2.4

COCO dataset with ImageBind embeddings, our adversarial hub was retrieved as the most relevant 21,918 times while the natural hub with the most retrievals was retrieved only 102 times: a $215\times$ gap in retrieval frequency. The retrieval frequency gap is smallest for the CUB-200-2011 dataset with OpenCLIP-ViT ($3.1\times$).

We clarify that the retrieval count for a natural hub should refer to the number of *irrelevant* user queries that retrieve the hub as the most relevant result, rather than the total number of queries that retrieve it, as some queries may be relevant. For instance, in the case of the CUB-200-2011 dataset using OpenCLIP-ViT (where the gap between natural and adversarial hubs is smallest), a natural hub is, on average, relevant to 28 user queries. Therefore, while some clean gallery points are retrieved by up to 100 queries and thus classified as natural hubs with 100 irrelevant retrievals, their actual number of irrelevant retrievals may be closer to $100 - 28 = 72$.

These results show that, adversarial hubs are much more severe threats than natural hubs. This threat will increase drastically if attackers are able to craft multiple (e.g., k) adversarial hubs to poison the gallery data.

5.3. Transferability of Universal Adversarial Hubs

In this section, we evaluate the transferability between different encoders, simulating a scenario where an attacker

lacks knowledge of the exact embedding method used by the victim retrieval system. Instead, the attacker leverages open-source embedding models to generate proxy adversarial hubs, which are then transferred to the victim’s embedding model. However, we note that our method primarily focuses on (and may overfit to) single embedding spaces, without prioritizing transferability. Exploring universally transferable adversarial hubs remains a promising direction for future research.

Table 4 shows how our attack transfers between different embedding models used by the attacker and the victim. In most cases, the adversarial hubs do not transfer, indicating a limited ability of adversarial features to generalize across models. These settings are omitted from Table 4. We find that OpenCLIP-ViT transfers effectively to ImageBind, achieving a high top-1 recall of $R@1 = 87.8\%$ and a median rank of $MdR = 1.0$. In contrast, adversarial hubs generated from OpenCLIP-RN50 barely transfer to AudioCLIP, with a top-1 recall of only $R@1 = 0.3\%$ and an $MdR = 416$, though still better than random chance (0.02%).

This observation aligns with previous work on illusions in multi-modal alignment [71], where adversarial illusions transfer within but not across similar model architectures. ImageBind adds modalities to an otherwise-unchanged ViT version of CLIP, which may indicate why OpenCLIP-ViT’s hubs transfer well. Meanwhile, AudioCLIP fine-tunes a ResNet-50-based CLIP, fundamentally altering the resul-

TABLE 2: Image-to-Image Retrieval (CUB-200-2011).

Model	Gallery	Retrieved	$R@1(\%)\uparrow$	$R@3(\%)\uparrow$	$R@5(\%)\uparrow$	$R@10(\%)\uparrow$	MdR \downarrow
ImageBind	Clean	Relevant Doc.	59.2	77.7	84.9	92.3	1.0
	Poisoned	Relevant Doc.	57.9 ± 0.2	75.8 ± 0.1	83.5 ± 0.1	91.3 ± 0.0	1.0 ± 0.0
	Poisoned	Adv. Hub	5.6 ± 0.5	39.8 ± 1.8	65.3 ± 2.0	90.3 ± 1.6	4.0 ± 0.1
AudioCLIP	Clean	Relevant Doc.	11.2	21.8	28.8	39.4	19.0
	Poisoned	Relevant Doc.	9.8 ± 0.3	20.5 ± 0.2	27.5 ± 0.1	38.3 ± 0.1	19.2 ± 0.3
	Poisoned	Adv. Hub	19.9 ± 2.6	40.4 ± 4.2	52.8 ± 4.4	71.0 ± 3.5	5.1 ± 0.9
OpenCLIP-ViT	Clean	Relevant Doc.	59.5	79.5	86.2	93.0	1.0
	Poisoned	Relevant Doc.	58.0 ± 0.1	77.5 ± 0.2	84.8 ± 0.1	92.3 ± 0.0	1.0 ± 0.0
	Poisoned	Adv. Hub	5.2 ± 0.5	39.3 ± 2.2	66.1 ± 2.2	92.3 ± 1.5	4.0 ± 0.2
OpenCLIP-RN50	Clean	Relevant Doc.	22.0	38.7	48.0	62.1	6.0
	Poisoned	Relevant Doc.	18.9 ± 0.4	35.8 ± 0.2	45.8 ± 0.1	60.4 ± 0.1	7.0 ± 0.1
	Poisoned	Adv. Hub	23.9 ± 2.8	50.9 ± 3.5	63.8 ± 2.9	81.0 ± 2.0	3.3 ± 0.5
AudioCLIP (Partial)	Clean	Relevant Doc.	12.1	22.2	28.3	38.9	19.0
	Poisoned	Relevant Doc.	11.2 ± 0.5	21.2 ± 0.4	27.6 ± 0.2	37.9 ± 0.2	19.9 ± 0.2
	Poisoned	Adv. Hub	11.5 ± 5.5	29.0 ± 9.9	41.8 ± 11.0	63.7 ± 10.2	7.3 ± 2.4
Pinecone	Clean	Relevant Doc.	25.6	41.5	51.5	-	-
	Poisoned	Relevant Doc.	25.2 ± 0.3	41.1 ± 0.3	51.1 ± 0.2	-	-
	Poisoned	Adv. Hub	11.0 ± 1.8	31.6 ± 4.2	45.7 ± 4.9	-	-

TABLE 3: Audio-to-Text Retrieval (Audiocaps).

Model	Gallery	Retrieved	$R@1(\%)\uparrow$	$R@5(\%)\uparrow$	$R@10(\%)\uparrow$	MdR \downarrow
ImageBind	Clean	Relevant Doc.	9.7	30.7	43.7	13.0
	Poisoned	Relevant Doc.	6.6 ± 0.5	28.1 ± 0.3	42.3 ± 0.1	14.0 ± 0.0
	Poisoned	Adv. Hub	53.2 ± 5.3	72.1 ± 5.5	82.1 ± 5.0	1.3 ± 0.7
AudioCLIP	Clean	Relevant Doc.	6.2	20.7	31.8	27.0
	Poisoned	Relevant Doc.	2.4 ± 0.8	18.8 ± 0.3	30.6 ± 0.2	28.0 ± 0.0
	Poisoned	Adv. Hub	59.0 ± 14.3	78.4 ± 10.5	86.5 ± 8.0	1.5 ± 0.9

TABLE 4: Transfer Results in Image-to-Text Retrieval (MS COCO). This table follows the same naming conventions and evaluation metrics as described in the caption of Table 1.

Target Model	Surrogate Model	Gallery	Retrieved	$R@1(\%)\uparrow$	$R@5(\%)\uparrow$	$R@10(\%)\uparrow$	MdR \downarrow
ImageBind	OpenCLIP-ViT	Poisoned	Relevant Doc.	9.1 ± 1.8	69.6 ± 0.0	79.8 ± 0.0	3.0 ± 0.1
		Poisoned	Adv. Hub	87.8 ± 2.7	95.8 ± 0.5	98.2 ± 0.3	1.0 ± 0.0
AudioCLIP (Partial)	OpenCLIP-RN50	Poisoned	Relevant Doc.	18.8 ± 0.0	39.5 ± 0.0	50.7 ± 0.0	10.0 ± 0.0
		Poisoned	Adv. Hub	0.3 ± 0.4	1.1 ± 1.5	2.1 ± 2.4	416.5 ± 244.1

tant embedding space. This likely contributes to the poor (but non-negligible) transferability from OpenCLIP-RN50’s hubs.

These results suggest that the architectural similarity between the surrogate and target models plays a crucial role in the success of adversarial transfer, and, given the limited number of open-source visual and audio encoders, it is easy to guess the architecture of the target embedding model. In addition, since different embedding models capture similar essential and invariant features, we purport that leveraging an ensemble of diverse surrogate models may lead to universally transferable adversarial hubs that avoid over-fitting to any single architecture [36], [56], [71].

5.4. Concept-Specific Adversarial Hubs

For our concept-specific hubs, we evaluate the text-to-image retrieval task on the MS COCO dataset with ImageBind. We first describe the generation process of the concept-specific queries as well as the concept-specific adversarial hubs. Then, we show their effectiveness.

Generation of Concept-specific Queries. From Zhang et al.’s [70] list of triggers, we start by randomly selecting 5 to use as concepts, ensuring that they do not appear in the text captions of MS COCO.

Then, for each concept c , we query ChatGPT-4o with the prompt “Generate 20 captions about images of (c)” to generate the concept-specific queries. Next, we split the 20 queries for each concept into two groups of 10. Starting from a randomly-selected clean gallery image, we use the first group to generate our

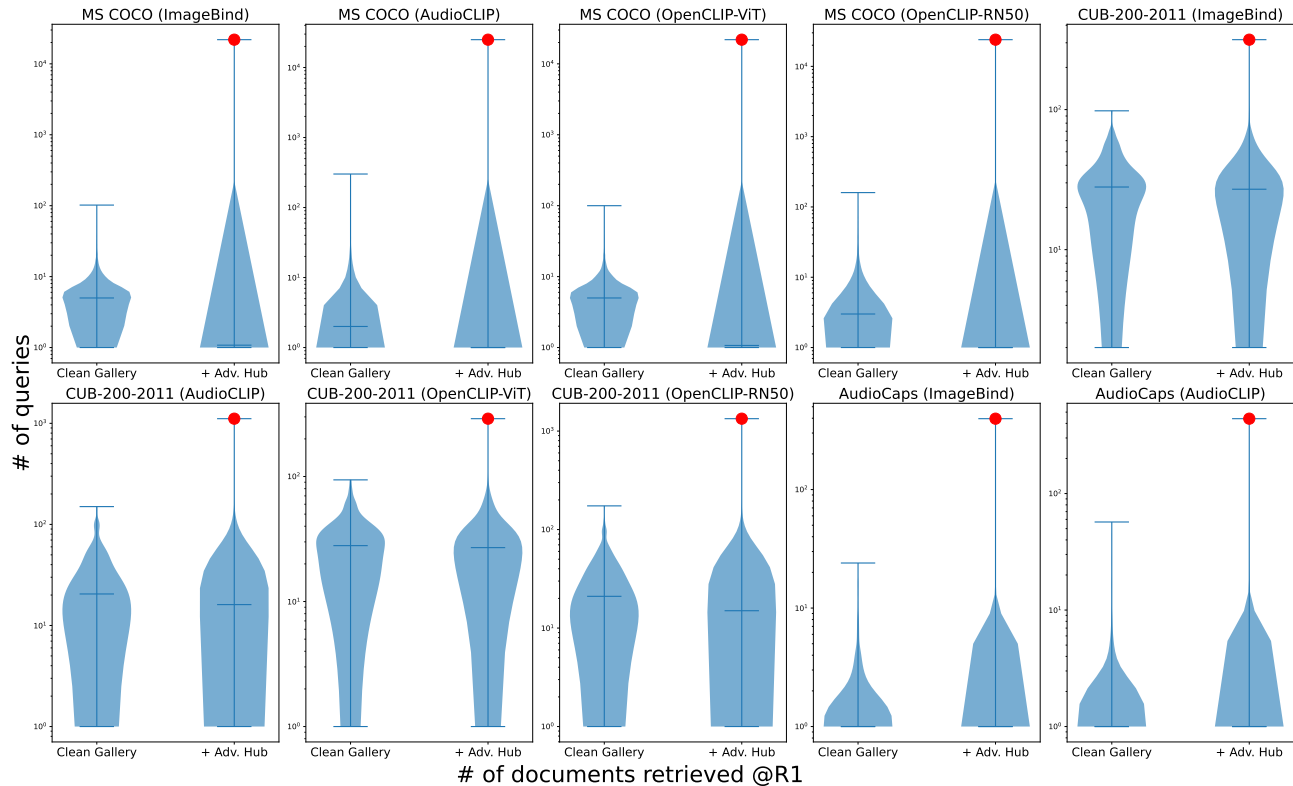


Figure 7: **Retrieval Frequency of Adversarial and Natural Hubs.** Adversarial hubs (red dots) are retrieved more frequently than the most relevant gallery points, including natural hubs. The width of each plot represents the frequency of retrieval across different numbers of queries (y-axis), shown on a logarithmic scale. The frequency of each gallery data point is an average over 100 independent adversarial hub generation trials.

TABLE 5: **Concept-specific Adversarial Hubs (MS COCO).** The gallery in this evaluation is the poisoned gallery with injected adversarial hub. In the column of “Query”, “Original” denotes the user queries irrelevant to the attacker-chosen concept and “Concept-specific” denotes the subset of queries that contain the concept.

Concept	Query	Retrieved	$R@1$ (%) \uparrow	$R@5$ (%) \uparrow	$R@10$ (%) \uparrow	MdR \downarrow
Amazon	Original	Relevant Doc.	48.4 \pm 0.0	72.7 \pm 0.0	81.0 \pm 0.0	2.0 \pm 0.0
	Original	Adv. Hub	0.1 \pm 0.0	0.8 \pm 0.4	1.6 \pm 0.8	211.4 \pm 67.7
	Concept-specific	Adv. Hub	100.0 \pm 0.0	100.0 \pm 0.0	100.0 \pm 0.0	1.0 \pm 0.0
LeBron James	Original	Relevant Doc.	48.1 \pm 0.1	72.5 \pm 0.1	80.9 \pm 0.0	2.0 \pm 0.0
	Original	Adv. Hub	1.3 \pm 0.7	6.1 \pm 3.0	10.9 \pm 5.0	73.5 \pm 25.8
	Concept-specific	Adv. Hub	100.0 \pm 0.0	100.0 \pm 0.0	100.0 \pm 0.0	1.0 \pm 0.0
Spotify	Original	Relevant Doc.	48.4 \pm 0.0	72.7 \pm 0.0	81.0 \pm 0.0	2.0 \pm 0.0
	Original	Adv. Hub	0.0 \pm 0.0	0.5 \pm 0.3	1.1 \pm 0.7	269.9 \pm 79.0
	Concept-specific	Adv. Hub	100.0 \pm 0.0	100.0 \pm 0.0	100.0 \pm 0.0	1.0 \pm 0.0
Olympics	Original	Relevant Doc.	45.0 \pm 1.3	71.7 \pm 0.3	80.5 \pm 0.1	2.0 \pm 0.0
	Original	Adv. Hub	13.8 \pm 4.3	33.0 \pm 9.0	44.3 \pm 10.5	16.4 \pm 8.8
	Concept-specific	Adv. Hub	100.0 \pm 0.0	100.0 \pm 0.0	100.0 \pm 0.0	1.0 \pm 0.0
Marilyn Monroe	Original	Relevant Doc.	48.3 \pm 0.1	72.6 \pm 0.0	81.0 \pm 0.0	2.0 \pm 0.0
	Original	Adv. Hub	0.3 \pm 0.1	3.1 \pm 1.2	6.1 \pm 2.3	118.1 \pm 27.8
	Concept-specific	Adv. Hub	100.0 \pm 0.0	100.0 \pm 0.0	100.0 \pm 0.0	1.0 \pm 0.0
Average	Original	Relevant Doc.	47.6 \pm 1.4	72.4 \pm 0.4	80.9 \pm 0.2	2.0 \pm 0.0
	Original	Adv. Hub	3.1 \pm 5.8	8.7 \pm 13.2	12.8 \pm 17.2	137.9 \pm 93.2
	Concept-specific	Adv. Hub	100.0 \pm 0.0	100.0 \pm 0.0	100.0 \pm 0.0	1.0 \pm 0.0

adversarial hub. The remaining 10 queries are used for evaluation. In this fashion, we generate 100 independent hubs for each of the 5 concepts.

Effectiveness of Concept-specific Hubs. Table 5 shows the effectiveness of our concept-specific adversarial hubs, designed to only target concept-specific queries. We first observe that the retrieval performance of the original 25,000 text queries on the poisoned gallery data (first row of each concept) is almost the same as the retrieval performance on the clean gallery data while the retrieval rate for adversarial hubs (second row) is nearly 0%. Meanwhile, our adversarial hubs are always retrieved by the relevant concept queries (third row): $R@1 = 100\%$ for all concepts and $MdR = 1$.

These results indicate that the concept-specific adversarial hubs are stealthy and effective, not only pinpointing concept queries, but also minimally impacting the remaining irrelevant queries. In Section 6, we further show that these are extremely hard to detect via current defenses against natural hubs, motivating further research into the design of defenses customized for adversarial hubs.

6. Evaluation of Existing Defenses

We first describe a representative defense against natural hubs [4] in Section 6.1. We then evaluate the effectiveness of this defense against our universal hubs in Section 6.2. Finally, we investigate how concept-based adversarial hubs circumvent these defenses in Section 6.3.

6.1. Query Bank Normalization Defense

High-level Idea of Defense. We first the high level idea of the defense proposed by Bogolin et al. [4]. Given a user query q , the defense aims to normalize the similarity score of the most relevant gallery data point if this similarity is suspected to be "abnormally" high. The defender begins by sampling a query bank Q_b from the same distribution as user queries (e.g., queries used for encoder training). Next, the defender identifies a subset of gallery data points as potential hubs and stores their indices in an activation set \mathcal{A} .

When a user query is received, the defender checks whether the index of the most relevant gallery point (based on cosine similarity) belongs to \mathcal{A} . If the index is not in \mathcal{A} , the similarity score remains unchanged. Otherwise, the defender suspects the corresponding gallery point to be a hub and normalizes its similarity score by dividing the original (cosine) similarity by the sum of its cosine similarities with the top- K most relevant queries from the query bank Q_b . Specifically, both the original cosine similarity and the similarities with the top- K queries from Q_b are scaled by a temperature parameter β before the normalization.

For the above procedure, the activation set \mathcal{A} is defined as:

$$\mathcal{A} = \{j : j \in \operatorname{argmax}_{g_j \in G}^k \operatorname{sim}(q_i, g_j), q_i \in Q_b\},$$

where $\operatorname{argmax}_{g_j \in G}^k$ returns the indices of the top- k most relevant gallery data points in $G = \{g_j\}_{j=1}^S$. Therefore, this activation set contains indices of gallery data that at least appears once as the top- k relevant points for queries in Q_b . Then a probe vector $p_j \in \mathbb{R}^K$ is precomputed for each gallery $g_j \in G$, which is composed of the cosine similarities with the top- K most relevant queries from Q_b . Note that the K can be different from the small k . Summation of their scaled (by β) entries will then be used to normalize the original high cosine similarity if this gallery data index is in \mathcal{A} .

Next, we show the more formal description about this normalization process. For notational convenience, for a query q , denote its similarity score with gallery point g_j as sim_j for clarity. Then, with \mathcal{A} and the given query q , the final normalized similarity score $\eta_q(j)$ of g_j in response to q is computed as:

$$\eta_q(j) = \begin{cases} \frac{\exp(\beta \cdot \operatorname{sim}_j)}{\mathbf{1}^T \exp([\beta \cdot p_j])} & \text{if } \operatorname{argmax}_{g_j \in G} \operatorname{sim}_j \in \mathcal{A} \\ \operatorname{sim}_j & \text{otherwise} \end{cases} \quad (3)$$

where β is a hyperparameter that controls the normalization temperature. This activation set \mathcal{A} is formed to mitigate abnormally high similarities while having minimal impact on other clean retrievals, as blindly normalizing similarities of all gallery data points with respect to the query q can negatively impact the clean retrieval performance [4].

We particularly study the defense by Bogolin et al. in this paper because it is the first scalable defense for modern cross-modal retrieval systems and subsequent works [13], [63] follow the same architecture, but makes minor variations on the query bank construction to improve efficiency, which has the potential risk of increasing the vulnerability to adversarial hubs (detailed discussions are added at the end of Section 6.2). For defense evaluation, we follow the default hyperparameter configurations in the original paper [4].

Lazy and Diligent Defenses. In modern retrieval systems, galleries can be massive and continuously updated (e.g., adding new products on e-commerce platforms). However, the precomputations required for the discussed defense can be extremely resource-intensive for systems with large galleries and query banks. As a result, it is likely that the system owner deploying the defense will perform these computations less frequently compared to the addition of new gallery items.

If an attacker carefully times their action and adds a single adversarial hub to the gallery after the precomputations for the current gallery and query bank data have been completed, the retrieval system may wait for some time before recomputing to account for the new additions. During this interval, the defense will effectively function as if no defense is in place, because the probe vector p_j of the adversarial hub will be zero, and the hub will not be included in the activation set \mathcal{A} . This makes our attack highly effective against such a *lazy* defense.

In the remaining sections, we consider a *diligent* defense, which promptly updates the probe vector and activation

set regardless of computational costs. While this approach ensures robustness, it may not be practical for real-world applications due to the significant resource demands.

6.2. Effectiveness of Universal Hubs Under Defense

We first evaluate the effectiveness of indiscriminate universal hubs generated without considering the defenses (oblivious attack). The evaluation is conducted on the MS COCO dataset using embeddings from ImageBind, with results shown in Table 6. Interestingly, we find that the defense has a disparate impact on the clean gallery data and the adversarial hub. For user queries, the retrieval performance on the original gallery data remains largely unchanged with or without defense. However, for the universal adversarial hub, the defense completely mitigates its impact: the top-1 recall drops from 76.6% without defense to 0% with defense, the top-10 recall decreases from 94% to around 9%, and the median rank increases from 1.3 to at least 700.

Given the effectiveness of this mitigation strategy, we proceed to test adaptive attacks against the defense to evaluate whether the (diligent) defense can still maintain its effectiveness.

Adaptive Attacks. We hypothesize that our oblivious adversarial hub (of the defense) is detected as a potential hub due to its frequent retrieval by query bank captions, which (ideally) share high similarity with normal user queries. As a result, the defense normalizes the hub and reduces its effectiveness. To circumvent this, we propose generating an adversarial hub that satisfies the following conditions: (1) it is dissimilar to the current query bank, either excluding the hub from \mathcal{A} or ensuring that the probe vector for the hub has lower similarity values; and (2) it remains close to the maximum possible number of user queries to maintain attack effectiveness. In essence, we aim to “overfit” the adversarial hub to the query bank samples, ensuring low similarity to them while maintaining high similarity to the user queries. This approach is feasible if the query bank samples and user queries are sufficiently complex, allowing for more flexibility in manipulating the adversarial hub’s features to achieve this “overfitting.”

Formally, we change our main objective from the primitive form in Equation (2) to the following contrastive form to account for being dissimilar to the query bank samples:

$$\begin{aligned} \mathcal{L}(g_a, Q; \theta) = & \alpha \frac{1}{|Q_b|} \sum_{b \in Q_b} \cos(\theta^{m_2}(g_a), \theta^{m_1}(b)) \\ & - \frac{1}{|Q_t|} \sum_{q \in Q_t} \cos(\theta^{m_2}(g_a), \theta^{m_1}(q)) \end{aligned} \quad (4)$$

where α is a hyperparameter that balances the two conditions (1) and (2).

Adaptive Attacks are Ineffective. In the formulation above, we assume the attacker is aware of the query bank Q_b . In practice, attackers may choose to generate proxy Q_b based on known representative user queries Q . We tried different

α values. However, even with this adaptive strategy and knowledge of Q_b , our adaptive attack still fails to generate an effective universal adversarial hub. The generated adversarial hubs either (1) are sufficiently close to user queries but are also similar to the query bank, and become irrelevant for user queries after normalization; or (2) become dissimilar to the query bank and avoid being normalized, but also distance themselves from the user queries, degrading the attack’s effectiveness. However, such a negative result may not always indicate the robustness of practical retrieval systems, as we elaborate further below.

Implication in Practice. Theoretically, the optimization in (4) involves two contradicting terms if Q_t and Q_b are sufficiently close to each other, causing the optimization to fail to converge. The objective becomes optimizable if the structure of queries Q_t and Q_b is complex, allowing the learning of features that distinguish samples from the two query sets. However, upon examining the text captions in the MS COCO dataset, we find that both Q_t and Q_b consist of high-level descriptions, reducing their distinguishability.

We anticipate that in practical applications, Q_t and Q_b may not be as similar as they are in the benchmark dataset. This aligns with prior findings suggesting that Q_b may not always be representative enough [4], [63]. In the next section, we show that when an attacker can easily target a subset of concept queries absent from Q_b , the generated concept-specific hubs can evade the defense, even without any adaptive contrastive optimization objectives.

Another important reason why modern retrieval systems may still be vulnerable to universal adversarial hubs is that the demonstrated defense is computationally expensive, as it relies on maintaining a very large Q_b to effectively represent potential user queries. In practice, developers might instead use only a small set of samples (e.g., k -nearest neighbors of the gallery data point in Q_b [13]) for normalization to reduce computational costs. However, this creates more opportunities for attackers due to the high asymmetry between the top- k samples in Q_b and the target queries Q_t (which is Q in this universal attack setting). As a result, the contrastive optimization in Equation (4) becomes significantly easier to solve. We leave the exploration of these settings as future work.

With the universal adversarial hubs evaluated under defense, we will next show how a defense-oblivious concept-specific attack can easily evade the current defenses.

6.3. Oblivious Concept-Specific Attacks

To better demonstrate the vulnerability of overly relying on the representativeness of Q_b to defend against adversarial hubs, we target a subset of concept queries that do not appear in Q_b . We do not adopt any advanced optimization techniques and instead use the same objective as in Equation (4). The attacker then uploads the single adversarial hub into the victim’s gallery data. The victim then (diligently) recomputes the probe vector and the activation set \mathcal{A} to normalize gallery data when needed (as per the condition

TABLE 6: **Universal Adversarial Hubs for Image-to-Text Retrieval with Query Bank Normalization Defense (MS COCO)**. In column of “QB-Norm”, “No” denotes the retrieval without defense, “Yes” denotes retrieval with defense based on query bank normalization.

Model	Gallery	Retrieved	QB-Norm	$R@1(\%)\uparrow$	$R@5(\%)\uparrow$	$R@10(\%)\uparrow$	MdR \downarrow
ImageBind	Clean	Relevant Doc.	No	48.4	72.7	81.0	2.0
	Clean	Relevant Doc.	Yes	49.9	73.8	82.3	2.0
	Poisoned	Relevant Doc.	No	9.2 \pm 2.1	69.6 \pm 0.0	79.8 \pm 0.0	3.0 \pm 0.0
	Poisoned	Relevant Doc.	Yes	49.7 \pm 0.0	74.2 \pm 0.0	82.6 \pm 0.0	2.0 \pm 0.1
	Poisoned	Adv. Hub	No	87.7 \pm 3.0	98.5 \pm 0.5	99.2 \pm 0.3	1.0 \pm 0.0
	Poisoned	Adv. Hub	Yes	0.0 \pm 0.0	9.7 \pm 2.0	10.3 \pm 2.1	707.4 \pm 49.7
AudioCLIP (Partial)	Clean	Relevant Doc.	No	18.8	39.5	50.7	10.0
	Clean	Relevant Doc.	Yes	26.6	49.9	61.4	6.0
	Poisoned	Relevant Doc.	No	8.2 \pm 3.6	36.8 \pm 0.4	49.2 \pm 0.2	11.0 \pm 0.1
	Poisoned	Relevant Doc.	Yes	26.7 \pm 0.1	50.3 \pm 0.2	62.0 \pm 0.3	5.1 \pm 0.2
	Poisoned	Adv. Hub	No	65.5 \pm 19.1	83.9 \pm 13.2	89.3 \pm 10.3	1.6 \pm 2.6
	Poisoned	Adv. Hub	Yes	0.0 \pm 0.0	6.2 \pm 1.5	7.6 \pm 2.0	1501.4 \pm 185.3

TABLE 7: **Concept-specific Adversarial Hubs with QB-Norm (MS COCO)**. The naming convention follows from Table 5. All retrievals are evaluated with defenses based on query-bank normalization.

Concept	Query	Retrieved	$R@1(\%)\uparrow$	$R@5(\%)\uparrow$	$R@10(\%)\uparrow$	MdR \downarrow
Amazon	Original	Relevant Doc.	49.9 \pm 0.0	73.8 \pm 0.0	82.3 \pm 0.0	2.0 \pm 0.0
	Original	Adv. Hub	0.0 \pm 0.0	0.4 \pm 0.2	0.8 \pm 0.4	662.0 \pm 58.0
	Concept-specific	Adv. Hub	100.0 \pm 0.0	100.0 \pm 0.0	100.0 \pm 0.0	1.0 \pm 0.0
LeBron James	Original	Relevant Doc.	49.9 \pm 0.1	73.8 \pm 0.0	83.2 \pm 0.0	2.0 \pm 0.0
	Original	Adv. Hub	0.0 \pm 0.0	2.1 \pm 1.0	4.0 \pm 1.8	615.0 \pm 42.6
	Concept-specific	Adv. Hub	100.0 \pm 0.0	100.0 \pm 0.0	100.0 \pm 0.0	1.0 \pm 0.0
Spotify	Original	Relevant Doc.	49.9 \pm 0.0	73.8 \pm 0.0	82.3 \pm 0.0	2.0 \pm 0.0
	Original	Adv. Hub	0.0 \pm 0.0	0.3 \pm 0.2	0.6 \pm 0.3	586.2 \pm 41.4
	Concept-specific	Adv. Hub	100.0 \pm 0.0	100.0 \pm 0.0	100.0 \pm 0.0	1.0 \pm 0.0
Olympics	Original	Relevant Doc.	49.8 \pm 0.0	73.8 \pm 0.0	82.3 \pm 0.0	2.0 \pm 0.0
	Original	Adv. Hub	0.0 \pm 0.0	9.1 \pm 2.7	13.8 \pm 3.4	683.4 \pm 97.4
	Concept-specific	Adv. Hub	93.4 \pm 4.0	99.9 \pm 0.7	100.0 \pm 0.5	1.0 \pm 0.0
Marilyn Monroe	Original	Relevant Doc.	49.9 \pm 0.0	73.8 \pm 0.0	82.3 \pm 0.0	2.0 \pm 0.0
	Original	Adv. Hub	0.0 \pm 0.0	1.4 \pm 0.5	2.7 \pm 0.9	572.5 \pm 39.4
	Concept-specific	Adv. Hub	100.0 \pm 0.0	100.0 \pm 0.0	100.0 \pm 0.0	1.0 \pm 0.0
Average	Original	Relevant Doc.	49.9 \pm 0.0	73.8 \pm 0.0	82.5 \pm 0.4	2.0 \pm 0.0
	Original	Adv. Hub	0.0 \pm 0.0	2.7 \pm 3.5	4.4 \pm 5.3	623.8 \pm 43.6
	Concept-specific	Adv. Hub	98.7 \pm 2.6	100.0 \pm 0.0	100.0 \pm 0.0	1.0 \pm 0.0

in Equation (3) for user queries. Results of this oblivious attack are shown in Table 7. From the table, we observe that in almost all cases, the top-1 recall is 100% for the adversarial hub when retrieved by the related concept queries, with a median rank of 1. Additionally, the original user queries rarely retrieve the adversarial hub under defense, indicating minimal collateral impact on irrelevant queries. The defense also has negligible impact on clean retrieval performance. These results highlight that the concept-specific attack is highly effective and stealthy, posing a significant challenge to defenses designed for natural hubness.

Potential Defenses. Under certain assumptions that are computationally challenging to satisfy in practice, current defenses may effectively mitigate indiscriminate universal adversarial hubs. However, our exploration of universal hubs is primarily aimed at benchmarking the overall performance of modern retrieval systems in adversarial environments, rather than focusing on their stealthiness. In real-world

scenarios, universal adversarial hubs may be easier to detect if they spam a large number of users, leading to common complaints. In contrast, concept-specific attacks pose a far greater practical threat. These attacks are both stealthy—avoiding detection through user feedback—and effective, maintaining their impact regardless of whether defenses are in place.

Our work calls on the research community to shift focus from mitigating natural hubs to addressing adversarial hubs, particularly concept-specific hubs. Several defense strategies from the adversarial machine learning literature may be worth exploring. For instance, data augmentation, which has proven effective against clean-label data poisoning attacks [5], could be applied to queries or gallery data in the cross-modal retrieval. However, the impact of data augmentation on clean retrieval performance remains unclear. Furthermore, when the adversarial hubs are reckless hubs, the effectiveness may also be limited, as data augmentations

mostly help for clean-label poisoning that adds bounded perturbations.

Other potential defenses include feature distillation techniques such as JPEG compression [37] or feature squeezing for images [66]. However, these methods can be circumvented by adaptive attacks [2]. Certified defenses based on techniques such as randomized smoothing may offer a more robust solution [14], and is worth exploring further.

7. Related Work

Adversarial Alignment and Adversarial Examples. The most relevant related work investigates *adversarial alignment* of inputs in multi-modal embedding spaces [18], [71]. These attacks incrementally adjust a malicious input to align with a *single target embedding* in an arbitrary modality. In contrast, adversarial hubs achieve the harder, universal goal of aligning a single input to a *large number of target embeddings* in arbitrary downstream modalities.

Our work builds on the broader literature on *untargeted* and *targeted* adversarial examples. Untargeted attacks cause outputs that are incorrect but not controlled by the adversary [22], while targeted attacks induce a specific, adversary-chosen, incorrect output [9]. In contrast, our approach seeks to generate adversarial inputs that work for *multiple targets at once* (dozens of thousands of queries in the case of multi-modal retrieval).

In this space, the most closely related papers are adversarial cross-modal examples [17], [20], [43], [53], [64], [73]. As well as being task-specific, these techniques only attack single targets. In other recent work [8], [44], [72], untargeted adversarial perturbations are used for jailbreaking and prompt injection in multi-modal chatbots.

Hoedt et al. [25] creates unimodal audio adversarial hubs for multiple targets in audio-to-audio retrieval, but the attack is limited to a handful of samples. Several other recent papers deploy unimodal adversarial examples against specific downstream tasks, such as toxicity classification [26], reading comprehension [29], and chatbots [76]. Furthermore, untargeted adversarial perturbations against contrastively-trained encoders are also demonstrated [32], [68], [75].

Importantly, unlike prior multi-target attacks, which induce different incorrect outputs for the same input across multiple models [33], and universal adversarial perturbations [41], which generalize across inputs rather than targets, our method operates against a single model but generalizes across embedding targets.

Poisoning Retrieval-Augmented Generation. Our work is also closely related to retrieval-augmented generation (RAG) poisoning, which involves an adversary who designs and injects adversarial documents into a RAG system’s corpus. In this setting, adversaries have two goals: (1) to create documents that are frequently retrieved (retrieval poisoning) and (2) to create documents that lead to unsafe generations when retrieved (generation poisoning).

Chaudhari et al. [10] studies trigger-based retrieval poisoning, where an attacker designs an adversarial document

that is retrieved for any query containing a specific trigger word. Meanwhile, others [67], [74] study trigger-less retrieval poisoning attacks by first clustering documents and then generating an adversarial document for each cluster. Zhang et al. [70] improves upon these methods by introducing a method to produce natural-looking text that works with both trigger and trigger-less setups. At the generation layer, attacks can produce adversarial documents that, when retrieved, cause generative models to produce harmful content or perform denial-of-service attacks [10], [52].

Notably, unlike our work, these approaches work with pure text-to-text retrieval systems. While our work is more closely related to the retrieval poisoning step, we observe that an adversary could also target generation *in any modality* by including malicious generation targets in their query set Q_t . We leave this exploration for future work.

Mitigation of Natural Hubness. Since hubs form organically in data distributions (*i.e.*, without adversarial manipulation), prior work focuses on mitigating *natural hubness*. There are two types of mitigation strategies for natural hubs: train-time [35] and post-processing methods [4], [49], [57], [63].

Train-time methods mitigate hubs by introducing hubness-aware loss functions [35] which downweight points that are close to multiple neighbors. While effective, these methods are costly for large models and have been mostly supplanted by post-processing methods, which rescale abnormally high similarities between points. Post-processing approaches are significantly more cost-efficient and well-studied. Early methods include some combination of local scaling [27], [49], [69], global scaling [25], [49], and centroid-scaling [24], [57], [58]. However, these methods are inefficient for large models. More scalable methods leverage a *query bank* as fixed reference points to normalize abnormal retrieval similarities [4], [13], [15], [16], [54], [63]. A few of these works explicitly address the cross-modal retrieval problem [4], [13], [63]. We discuss the efficacy of these methods against adversarial hubs in Section 6.

8. Conclusion and Possible Future Directions

In this paper, we revisit the well-known phenomenon of hubness, where a data point in a high-dimensional space can appear in the neighborhood of many other points that are semantically not related, and investigate how it can be exploited for adversarial purposes in multi-modal retrieval systems.

We introduce two types of adversarial hubs, universal hubs that are close to and thus retrieved by many irrelevant user queries, and concept-specific hubs that are only retrieved by queries corresponding to specific, attacker-chosen concepts. Through empirical evaluations, we show that adversarial hubs can be crafted to appear relevant to many more queries than natural hubs. This implies that adversarial hubs can be potentially used for spam and product promotion attacks on modern multi-modal retrieval systems that rely on pretrained embeddings. Furthermore, we show that current defenses designed to mitigate natural hubness

are ineffective against concept-based adversarial hubs. We hope that our results will motivate research on more effective defenses against adversarial hubs.

An interesting direction for future research is to investigate local perturbations, similar to adversarial patches [6], that can be applied to any image to generate adversarial hubs. While this paper focused on image and audio adversarial hubs, similar techniques could be extended to other modalities, such as video or thermal images, provided the multi-modal encoder supports these inputs.

Another question for future research is measuring how does adversarial hubness affect the performance of multi-modal RAG systems, which also have broader application scenarios [65].

On the defense side, developers of multi-modal embedding systems need to understand how their models can be exploited for attacks and how adversarial hubs can expose users of retrieval systems to risks, such as misinformation or spam. Developing robust defenses against these types of adversarial threats should be a key focus moving forward, and we discussed several possible approaches in Section 6.3.

Ethical Considerations

While our work investigates the vulnerability of multi-modal retrieval systems to adversarial hubs, our primary goal is to raise awareness within the community about these threats and to inspire the development of effective defenses against adversarial hubs.

Acknowledgments

Supported in part by the NSF grant 2311521 and the Google Cyber NYC Institutional Research Program.

References

- [1] "Pinecone - vector database for machine learning," <https://www.pinecone.io>, accessed: 2024-11-12.
- [2] A. Athalye, N. Carlini, and D. Wagner, "Obfuscated gradients give a false sense of security: Circumventing defenses to adversarial examples," in *International conference on machine learning*. PMLR, 2018, pp. 274–283.
- [3] K. Barnard, P. Duygulu, D. Forsyth, N. De Freitas, D. M. Blei, and M. I. Jordan, "Matching words and pictures," *The Journal of Machine Learning Research*, vol. 3, pp. 1107–1135, 2003.
- [4] S.-V. Bogolin, I. Croitoru, H. Jin, Y. Liu, and S. Albanie, "Cross modal retrieval with querybank normalisation," in *Proceedings of the IEEE/CVF Conference on Computer Vision and Pattern Recognition (CVPR)*, 2022.
- [5] E. Borgnia, V. Cherepanova, L. Fowl, A. Ghiasi, J. Geiping, M. Goldblum, T. Goldstein, and A. Gupta, "Strong data augmentation sanitizes poisoning and backdoor attacks without an accuracy tradeoff," in *ICASSP 2021-2021 IEEE International Conference on Acoustics, Speech and Signal Processing (ICASSP)*, 2021.
- [6] T. B. Brown, D. Mané, A. Roy, M. Abadi, and J. Gilmer, "Adversarial patch," *arXiv:1712.09665*, 2017.
- [7] N. Carlini, M. Jagielski, C. A. Choquette-Choo, D. Paleka, W. Pearce, H. Anderson, A. Terzis, K. Thomas, and F. Tramèr, "Poisoning web-scale training datasets is practical," in *IEEE Symposium on Security and Privacy (S&P)*, 2024.
- [8] N. Carlini, M. Nasr, C. A. Choquette-Choo, M. Jagielski, I. Gao, A. Awadalla, P. W. Koh, D. Ippolito, K. Lee, F. Tramèr, and L. Schmidt, "Are aligned neural networks adversarially aligned?" *arXiv:2306.15447*, 2023.
- [9] N. Carlini and D. Wagner, "Audio adversarial examples: Targeted attacks on speech-to-text," in *IEEE Symposium on Security and Privacy Workshops*, 2018.
- [10] H. Chaudhari, G. Severi, J. Abascal, M. Jagielski, C. A. Choquette-Choo, M. Nasr, C. Nita-Rotaru, and A. Oprea, "Phantom: General trigger attacks on retrieval augmented language generation," *arXiv preprint arXiv:2405.20485*, 2024.
- [11] X. Chen, H. Fang, T.-Y. Lin, R. Vedantam, S. Gupta, P. Dollár, and C. L. Zitnick, "Microsoft coco captions: Data collection and evaluation server," *arXiv:1504.00325*, 2015.
- [12] M. Cherti, R. Beaumont, R. Wightman, M. Wortsman, G. Ilharco, C. Gordon, C. Schuhmann, L. Schmidt, and J. Jitsev, "Reproducible scaling laws for contrastive language-image learning," in *Proceedings of the IEEE/CVF Conference on Computer Vision and Pattern Recognition (CVPR)*, 2023.
- [13] N. Chowdhury, F. Wang, S. Shenoy, D. Kiela, S. Schwettmann, and T. Thrush, "Nearest neighbor normalization improves multimodal retrieval," in *Proceedings of the 2024 Conference on Empirical Methods in Natural Language Processing (EMNLP)*, 2024.
- [14] J. Cohen, E. Rosenfeld, and Z. Kolter, "Certified adversarial robustness via randomized smoothing," in *international conference on machine learning*. PMLR, 2019, pp. 1310–1320.
- [15] A. Conneau, G. Lample, M. Ranzato, L. Denoyer, and H. Jégou, "Word translation without parallel data," *International Conference on Learning Representations (ICLR)*, 2018.
- [16] G. Dinu, A. Lazaridou, and M. Baroni, "Improving zero-shot learning by mitigating the hubness problem," *arXiv:1412.6568*, 2014.
- [17] Y. Dong, H. Chen, J. Chen, Z. Fang, X. Yang, Y. Zhang, Y. Tian, H. Su, and J. Zhu, "How robust is google's bard to adversarial image attacks?" in *R0-FoMo: Robustness of Few-shot and Zero-shot Learning in Large Foundation Models*, 2023.
- [18] Z. Dou, X. Hu, H. Yang, Z. Liu, and M. Fang, "Adversarial attacks to multi-modal models," *arXiv preprint arXiv:2409.06793*, 2024.
- [19] A. Flexer, M. Dörfler, J. Schlüter, and T. Grill, "Hubness as a case of technical algorithmic bias in music recommendation," in *2018 IEEE International Conference on Data Mining Workshops (ICDMW)*, 2018.
- [20] K. Gao, Y. Bai, J. Bai, Y. Yang, and S.-T. Xia, "Adversarial robustness for visual grounding of multimodal large language models," in *ICLR 2024 Workshop on Reliable and Responsible Foundation Models*, 2024.
- [21] R. Girdhar, A. El-Nouby, Z. Liu, M. Singh, K. V. Alwala, A. Joulin, and I. Misra, "ImageBind: One embedding space to bind them all," in *IEEE/CVF Conference on Computer Vision and Pattern Recognition (CVPR)*, 2023.
- [22] I. J. Goodfellow, J. Shlens, and C. Szegedy, "Explaining and harnessing adversarial examples," in *International Conference on Learning Representations (ICLR)*, 2015.
- [23] A. Guzhov, F. Raue, J. Hees, and A. Dengel, "AudioCLIP: Extending CLIP to image, text and audio," in *IEEE International Conference on Acoustics, Speech and Signal Processing (ICASSP)*, 2022.
- [24] K. Hara, I. Suzuki, M. Shimbo, K. Kobayashi, K. Fukumizu, and M. Radovanović, "Localized centering: Reducing hubness in large-sample data," in *Proceedings of the AAAI Conference on Artificial Intelligence (AAAI)*, 2015.
- [25] K. Hoedt, A. Flexer, and G. Widmer, "Defending a music recommender against hubness-based adversarial attacks," in *Proceedings of the 19th Sound and Music Computing Conference (SMC)*, 2022.

- [26] H. Hosseini, S. Kannan, B. Zhang, and R. Poovendran, “Deceiving Google’s perspective API built for detecting toxic comments,” *arXiv:1702.08138*, 2017.
- [27] H. Jegou, H. Harzallah, and C. Schmid, “A contextual dissimilarity measure for accurate and efficient image search,” in *IEEE/CVF Conference on Computer Vision and Pattern Recognition (CVPR)*, 2007.
- [28] J. Jeon, V. Lavrenko, and R. Manmatha, “Automatic image annotation and retrieval using cross-media relevance models,” in *Proceedings of the 26th annual international ACM SIGIR conference on Research and development in information retrieval (SIGIR)*, 2003.
- [29] R. Jia and P. Liang, “Adversarial examples for evaluating reading comprehension systems,” in *Conference on Empirical Methods in Natural Language Processing (EMNLP)*, 2017.
- [30] A. Kerckhoffs, *La cryptographie militaire*. BoD—Books on Demand, 2023.
- [31] C. D. Kim, B. Kim, H. Lee, and G. Kim, “AudioCaps: Generating captions for audios in the wild,” in *Proceedings of the 2019 Conference of the North American Chapter of the Association for Computational Linguistics: Human Language Technologies (NAACL)*, 2019.
- [32] M. Kim, J. Tack, and S. J. Hwang, “Adversarial self-supervised contrastive learning,” in *Annual Conference on Neural Information Processing Systems (NeurIPS)*, 2020.
- [33] H. Kwon, Y. Kim, K.-W. Park, H. Yoon, and D. Choi, “Multi-targeted adversarial example in evasion attack on deep neural network,” *IEEE Access*, vol. 6, pp. 46 084–46 096, 2018.
- [34] A. Lazaridou, G. Dinu, and M. Baroni, “Hubness and pollution: Delving into cross-space mapping for zero-shot learning,” in *Proceedings of the 53rd Annual Meeting of the Association for Computational Linguistics (ACL)*, 2015.
- [35] F. Liu, R. Ye, X. Wang, and S. Li, “HAL: Improved text-image matching by mitigating visual semantic hubs,” in *Proceedings of the AAAI conference on artificial intelligence (AAAI)*, 2020.
- [36] Y. Liu, X. Chen, C. Liu, and D. Song, “Delving into transferable adversarial examples and black-box attacks,” in *International Conference on Learning Representations (ICLR)*, 2022.
- [37] Z. Liu, Q. Liu, T. Liu, N. Xu, X. Lin, Y. Wang, and W. Wen, “Feature distillation: Dnn-oriented jpeg compression against adversarial examples,” in *2019 IEEE/CVF Conference on Computer Vision and Pattern Recognition (CVPR)*, 2019.
- [38] T. Low, C. Borgelt, S. Stober, and A. Nürnberger, “The hubness phenomenon: Fact or artifact?” *Towards Advanced Data Analysis by Combining Soft Computing and Statistics*, pp. 267–278, 2013.
- [39] D. G. Lowe, “Distinctive image features from scale-invariant keypoints,” *International journal of computer vision*, vol. 60, pp. 91–110, 2004.
- [40] A. Madry, A. Makelov, L. Schmidt, D. Tsipras, and A. Vladu, “Towards deep learning models resistant to adversarial attacks,” in *International Conference on Learning Representations (ICLR)*, 2018.
- [41] S.-M. Moosavi-Dezfooli, A. Fawzi, O. Fawzi, and P. Frossard, “Universal adversarial perturbations,” in *Proceedings of the IEEE Conference on Computer Vision and Pattern Recognition (CVPR)*, July 2017.
- [42] A. v. d. Oord, Y. Li, and O. Vinyals, “Representation learning with contrastive predictive coding,” *arXiv:1807.03748*, 2018.
- [43] R. Peri, S. M. Jayanthi, S. Ronanki, A. Bhatia, K. Mundnich, S. Dingliwal, N. Das, Z. Hou, G. Huybrechts, S. Vishnubhotla *et al.*, “SpeechGuard: Exploring the adversarial robustness of multimodal large language models,” *arXiv preprint arXiv:2405.08317*, 2024.
- [44] X. Qi, K. Huang, A. Panda, M. Wang, and P. Mittal, “Visual adversarial examples jailbreak aligned large language models,” in *International Conference on Machine Learning (ICML) Workshop on New Frontiers in Adversarial Machine Learning*, 2023.
- [45] A. Radford, J. W. Kim, C. Hallacy, A. Ramesh, G. Goh, S. Agarwal, G. Sastry, A. Askell, P. Mishkin, J. Clark *et al.*, “Learning transferable visual models from natural language supervision,” in *International conference on machine learning (ICML)*, 2021.
- [46] M. Radovanovic, A. Nanopoulos, and M. Ivanovic, “Hubs in space: Popular nearest neighbors in high-dimensional data,” *Journal of Machine Learning Research (JMLR)*, vol. 11, no. 9, pp. 2487–2531, 2010.
- [47] G. Salton and C. Buckley, “Term-weighting approaches in automatic scaling retrieval,” *Information processing & management*, vol. 24, no. 5, pp. 513–523, 1988.
- [48] A. Salvador, N. Hynes, Y. Aytar, J. Marin, F. Ofli, I. Weber, and A. Torralba, “Learning cross-modal embeddings for cooking recipes and food images,” in *Proceedings of the IEEE conference on computer vision and pattern recognition (CVPR)*, 2017.
- [49] D. Schnitzer, A. Flexer, M. Schedl, and G. Widmer, “Local and global scaling reduce hubs in space,” *Journal of Machine Learning Research (JMLR)*, vol. 13, pp. 2871–2902, 2012.
- [50] F. Schroff, D. Kalenichenko, and J. Philbin, “FaceNet: A unified embedding for face recognition and clustering,” in *Proceedings of the IEEE conference on computer vision and pattern recognition (CVPR)*, 2015.
- [51] A. Shafahi, W. R. Huang, M. Najibi, O. Suciu, C. Studer, T. Dumitras, and T. Goldstein, “Poison frogs! targeted clean-label poisoning attacks on neural networks,” in *Proceedings of the 32nd International Conference on Neural Information Processing Systems (NeurIPS)*, 2018.
- [52] A. Shafan, R. Schuster, and V. Shmatikov, “Machine against the RAG: Jamming retrieval-augmented generation with blocker documents,” *arXiv:2406.05870*, 2024.
- [53] E. Shayegani, Y. Dong, and N. Abu-Ghazaleh, “Plug and Pray: Exploiting off-the-shelf components of multi-modal models,” *arXiv:2307.14539*, 2023.
- [54] S. L. Smith, D. H. Turban, S. Hamblin, and N. Y. Hammerla, “Offline bilingual word vectors, orthogonal transformations and the inverted softmax,” in *International Conference on Learning Representations (ICLR)*, 2017.
- [55] Spotify for Artists, “Artificial streaming,” 2023, accessed: 2024-11-13. [Online]. Available: <https://artists.spotify.com/artificial-streaming>
- [56] F. Suya, J. Chi, D. Evans, and Y. Tian, “Hybrid batch attacks: Finding black-box adversarial examples with limited queries,” in *29th USENIX Security Symposium (USENIX Security 20)*, 2020, pp. 1327–1344.
- [57] I. Suzuki, K. Hara, M. Shimbo, Y. Matsumoto, and M. Saerens, “Investigating the effectiveness of laplacian-based kernels in hub reduction,” in *Proceedings of the AAAI Conference on Artificial Intelligence (AAAI)*, 2012.
- [58] I. Suzuki, K. Hara, M. Shimbo, M. Saerens, and K. Fukumizu, “Centering similarity measures to reduce hubs,” in *Proceedings of the 2013 conference on empirical methods in natural language processing (EMNLP)*, 2013.
- [59] C. Szegedy, “Intriguing properties of neural networks,” in *International Conference on Learning Representations (ICLR)*, 2014.
- [60] C. Wah, S. Branson, P. Welinder, P. Perona, and S. Belongie, “The caltech-ucsd birds-200-2011 dataset,” 2011.
- [61] B. Wang, Y. Yang, X. Xu, A. Hanjalic, and H. T. Shen, “Adversarial cross-modal retrieval,” in *Proceedings of the 25th ACM international conference on Multimedia (ACM MM)*, 2017.
- [62] K. Wang, Q. Yin, W. Wang, S. Wu, and L. Wang, “A comprehensive survey on cross-modal retrieval,” *arXiv:1607.06215*, 2016.
- [63] Y. Wang, X. Jian, and B. Xue, “Balance Act: Mitigating hubness in cross-modal retrieval with query and gallery banks,” in *Proceedings of the 2023 Conference on Empirical Methods in Natural Language Processing (EMNLP)*, 2023.

- [64] C. H. Wu, J. Y. Koh, R. Salakhutdinov, D. Fried, and A. Raghunathan, “Adversarial attacks on multimodal agents,” *arXiv:2406.12814*, 2024.
- [65] P. Xia, K. Zhu, H. Li, H. Zhu, Y. Li, G. Li, L. Zhang, and H. Yao, “Rule: Reliable multimodal rag for factuality in medical vision language models,” *arXiv preprint arXiv:2407.05131*, 2024.
- [66] W. Xu, “Feature squeezing: Detecting adversarial examples in deep neural networks,” *arXiv preprint arXiv:1704.01155*, 2017.
- [67] J. Xue, M. Zheng, Y. Hu, F. Liu, X. Chen, and Q. Lou, “BadRAG: Identifying vulnerabilities in retrieval augmented generation of large language models,” *arXiv:2406.00083*, 2024.
- [68] Q. Yu, J. Lou, X. Zhan, Q. Li, W. Zuo, Y. Liu, and J. Liu, “Adversarial contrastive learning via asymmetric InfoNCE,” in *European Conference on Computer Vision (ECCV)*, 2022.
- [69] L. Zelnik-Manor and P. Perona, “Self-tuning spectral clustering,” in *Proceedings of the 17th International Conference on Neural Information Processing Systems (NeurIPS)*, 2004.
- [70] C. Zhang, T. Zhang, and V. Shmatikov, “Controlled generation of natural adversarial documents for stealthy retrieval poisoning,” *arXiv:2410.02163*, 2024.
- [71] T. Zhang, R. Jha, E. Bagdasaryan, and V. Shmatikov, “Adversarial illusions in multi-modal embeddings,” in *33rd USENIX Security Symposium (USENIX Security)*, 2024.
- [72] T. Zhang, C. Zhang, J. X. Morris, E. Bagdasarian, and V. Shmatikov, “Soft prompts go hard: Steering visual language models with hidden meta-instructions,” *arXiv:2407.08970*, 2024.
- [73] Y. Zhao, T. Pang, C. Du, X. Yang, C. Li, N.-M. Cheung, and M. Lin, “On evaluating adversarial robustness of large vision-language models,” in *Annual Conference on Neural Information Processing Systems (NeurIPS)*, 2023.
- [74] Z. Zhong, Z. Huang, A. Wettig, and D. Chen, “Poisoning retrieval corpora by injecting adversarial passages,” in *Proceedings of the 2023 Conference on Empirical Methods in Natural Language Processing (EMNLP)*, 2023, pp. 13 764–13 775.
- [75] Z. Zhou, S. Hu, R. Zhao, Q. Wang, L. Y. Zhang, J. Hou, and H. Jin, “Downstream-agnostic adversarial examples,” in *IEEE International Conference on Computer Vision (ICCV)*, 2023.
- [76] A. Zou, Z. Wang, J. Z. Kolter, and M. Fredrikson, “Universal and transferable adversarial attacks on aligned language models,” *arXiv:2307.15043*, 2023.
- [77] W. Zou, R. Geng, B. Wang, and J. Jia, “PoisonedRAG: Knowledge corruption attacks to retrieval-augmented generation of large language models,” *arXiv:2402.07867*, 2024.